Final Report

Project Title: Characterizing Spotted Owl Habitat Using LiDAR
Cooperative Agreement: P17AC01530
Prepared by: University of Washington, Forest Resilience Lab
Contact: Van R. Kane, vkane@uw.edu

April 14, 2019

Introduction

This report summarizes the results of the University of Washington's (UW) analysis regarding the characterization of spotted owl habitat use through the application of light detection and ranging (lidar) data. The methodology and results presented were conducted following coordination and consultation with Yosemite National Park and the Point Reyes Bird Observatory to integrate the methodology and results reported here to characterize CSO habitat in burned and unburned areas, before and after the 2013 Rim Fire. The UW was responsible for achieving the following deliverables, which are described herein:

1. produce lidar metrics from the 2013 Rim Fire lidar acquisition, as described below;
2. acquire Landsat images to develop Normalized Difference Vegetation and Normalized Burn Ratio Indices and incorporating these data into analyses to characterize CSO habitat;
3. conduct niche overlap modeling to identify canopy metrics relevant to characterizing CSO habitat in Yosemite; and
4. develop a raster layer of potential CSO habitat.

This report details the methods and results of to produce these deliverables. Discussion of the interpretation of these results will be incorporated into the report for the larger study being conducted by Yosemite.

Statement of Completeness

This final report details the methodology and work products that were completed per the agreement. All of the objectives of the agreement were completed as required and as detailed below within the allocated budget.

Methodology

Data Description, Preparation, and Analysis

This comparative analysis of the available and used habitat within the range of California Spotted Owl, *Strix occidentalis* (CSO) in Yosemite National Park (Yosemite) included examining the portion of the 2013 Rim Fire area in Yosemite to the unburned portion of the range in Yosemite, pre and post fire, using remotely sensed data. The range of the CSO in Yosemite is the land area identified as Mixed Conifer Forest according to the California Wildlife Habitat Relationship System[1]. For the purposes of the analytical steps included below, the niche overlap modeling was conducted on all locations within five

[1] https://www.wildlife.ca.gov/data/cwhr

km of any reported owl location (i.e. nesting and/or roosting) and the mapping of potential habitat was conducted over the entire Park boundary.

Lidar Data

Following the conclusion of the Rim fire on October 24, 2013, an airborne lidar acquisition was conducted over the burn area and an additional 2km buffer in November 2013. The data were collected by the National Center for Airborne Laser Mapping (NCALM), University of Houston, with an Optech Gemini Airborne Laser Mapper. The data were acquired at four returns per pulse, with a resolution of 12 points per meter squared; a scan angel of ± 14°; and a minimum 50% overlap in flight lines. Next, the lidar data were processed with the US Forest Service's Fusion software package (Mcgaughey, 2018) to create the canopy structure, canopy intensity (as a proxy for burn severity), as well as the topographic metrics that are averaged to a 90m pixel size, which were normalized to ensure all laser returns were of a height above the digital terrain model and provided in raster format, which also included the canopy area and large gap metrics.

Landsat Data

Landsat data were downloaded to provide metrics for the entire range of the CSO in Yosemite for pre and post fire, 2013 and 2014 as the lidar data only captured the post-fire portion of range affected by the Rim Fire. The Landsat metrics that were included were; canopy cover and height, topography (aspect, elevation, and slope), and relative differenced normalized burn ratio (corresponding to the lidar intensity). The Landsat data was also acquired to calculate the normalized difference of vegetation index (NDVI) for 2013 and 2014, which cannot be measured with airborne lidar data exclusively. All of the Landsat data were downloaded from the USGS Earth Explorer website[2] at a resolution of 90 meter in raster format.

Analysis

As the presence of California Spotted Owls are correlated with the cover of tall trees (North et al., 2017), the mapping of available and used nesting habitat, pre and post fire, was evaluated following the methods of North et al. 2017 by applying niche overlap modeling for each of the canopy structure, topographic, Relative differenced Normalized Burn Ratio (RdNBR), and Normalized Difference in Vegetation Index (NDVI) for 2013 and 2014 metrics within the occupied nest (diameter=112.8m), associated core areas (diameter=700m), and the range outside of the core areas. First, the Landsat and lidar-based metrics were brought into ESRI's ArcMap, Version 10.3.1[3] and visually inspected for accuracy prior to initiating the analysis in R-Studio, Version 1.1.419. Next, each of the Landsat and lidar-based metrics was projected to UTM, Zone 10N aligned, and clipped to the study area. After the values of each metric were added to new a data frame, niche overlap modeling was conducted for all the lidar-based and eight Landsat-based metrics (Table 1) to aid in the selection of suitable metrics. Niche overlap measures the similarity of two distributions, as a value between 0 and 1, 0 being no similarity, 1 being complete similarity. In this scenario we compared the distribution of known used owl habitat with available habitat which was defined as the whole landscape within 5km of any nest. This range was used to excluded landscape that is not available (i.e. different ecotype, etc.) and keep the focus on areas that owls had real potential to access. In our case a lower niche overlap value indicates the used habitat is different from the available (or that the owls exhibit a preference with regard to this metric) and that it might be a good metric to indicate owl habitat. The metrics selected for the lidar and Landsat based metrics are highlighted in blue in Table 1; the selected metrics included canopy area and height metrics

[2] https://earthexplorer.usgs.gov/
[3] ESRI software version 2.2: https://pro.arcgis.com/en/pro-app/

as well as burn severity, NDVI, slope, aspect and elevation. A cold-air pooling layer acquired from Dr. Jessica Lundquist, University of Washington, was analyzed with the niche-overlap modeling; however, no correlation with used nesting locations was observed. The cold-air pooling layer was a coarser resolution than the lidar or Landsat derived metrics (as it only indicated an area as exhibit pooling, some pooling, or no pooling), and the determination was made to exclude this variable from further analysis (it is not included in Table 1).

Following the niche-overlap modeling, the mean values of the nine nesting locations in the Rim fire footprint of Yosemite for each of the selected metrics was applied to conservatively identify "available" habitat. For each metric, available habitat was identified through a neighboring window analysis in R-studio. This analysis identified a 30mx30m pixel as suitable habitat (in a Boolean fashion) if its associated circular window (r = 700m), had a mean value above the 10th percentile and below the 90th percentile of the distribution for mean values of observed nests, for each of the selected metrics. The only selected metric where this methodology was not applied was the percent canopy area in the height class of greater than 48m. For this metric, a pixel was considered suitable as long as its value was above the 10th percentile alone. Raster layers were created for each selected metric that delineated available and used nesting habitat as described, and these layers were intersected (using a 'logical and' operation) to identify areas that have similar structure as known habitat for the range of CSO in Yosemite in the burned and unburned area. In order to be identified as potential available habitat, the location for each of the metrics had to be mapped as available.

Results

The results of the niche overlap modeling for the selected metrics by distance away from the nests for the lidar and Landsat based metrics are in Figures 1 and 2, respectively. Violin plots were created to display the frequency of the range of values for the selected lidar and Landsat based metrics for the nine nesting locations in the Rim fire portion of Yosemite compared to 10,000 randomly selected 'nest windows' identified as "available", Figure 3. Finally, a map layer of the potential available habitat was created, which may be viewed in ArcMap or R-studio.

Deliverables

1. The 2013 and 2014 Landsat image data was provided to Lynn Schofield in October 2018 via a 1TB external hardrive via standard mail.
2. The lidar metrics and associated raster products produced as a result of the analyses as described above are available for download at the following **dropbox.com location:** https://www.dropbox.com/sh/asbimixh6n6pfwa/AACiWVuqW28SIxacdnB-iAq6a?dl=0
3. The niche overlay modeling decay curves are provided in Figures 1 and 2, and the violin plot of nesting locations compared to randomly selected locations within the potential available habitat are depicted in Figure 3.

Literature Cited

Mcgaughey, R.J., 2018. FUSION / LDV : Software for LIDAR Data Analysis and Visualization.

North, M.P., Kane, J.T., Kane, V.R., Asner, G.P., Berigan, W., Churchill, D.J., Conway, S., Gutiérrez, R.J., Jeronimo, S., Keane, J., Koltunov, A., Mark, T., Moskal, M., Munton, T., Peery, Z., Ramirez, C., Sollmann, R., White, A.M., Whitmore, S., 2017. Cover of tall trees best predicts California spotted owl habitat. For. Ecol. Manage. 405, 166–178. https://doi.org/10.1016/j.foreco.2017.09.019

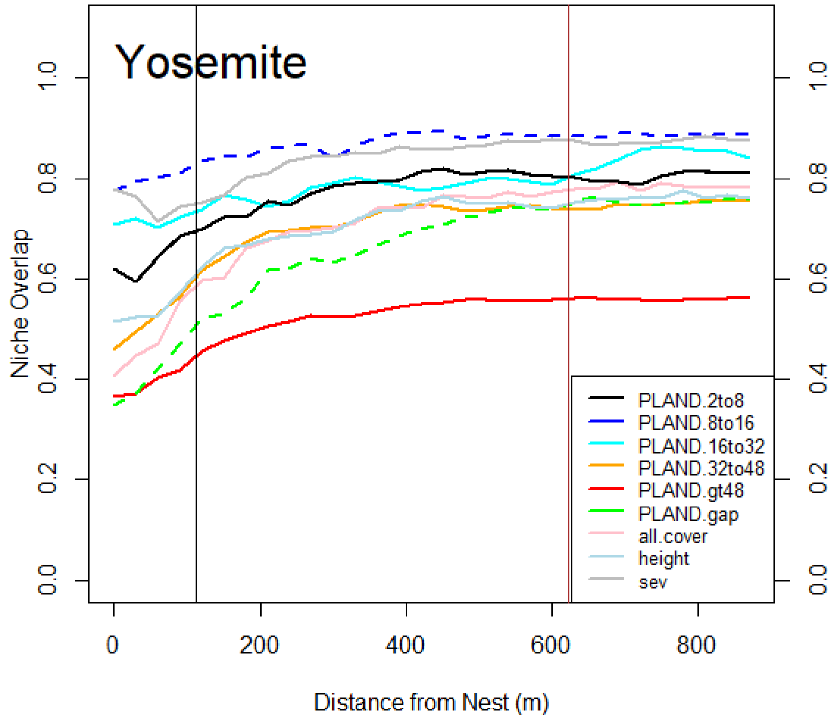

Figure 1: Niche-overlap modeling results for the post-fire, lidar-based metrics *Niche overlap as a function of distance from nest. The black vertical line represents the nest distance for an owl (112.8m) which was imputed as a function of latitidue from the nest distances in North et. al. 2017. The brown line represents the area of heavy utilization (700m). PLAND = Percent of Landscape in canopy height strata.*

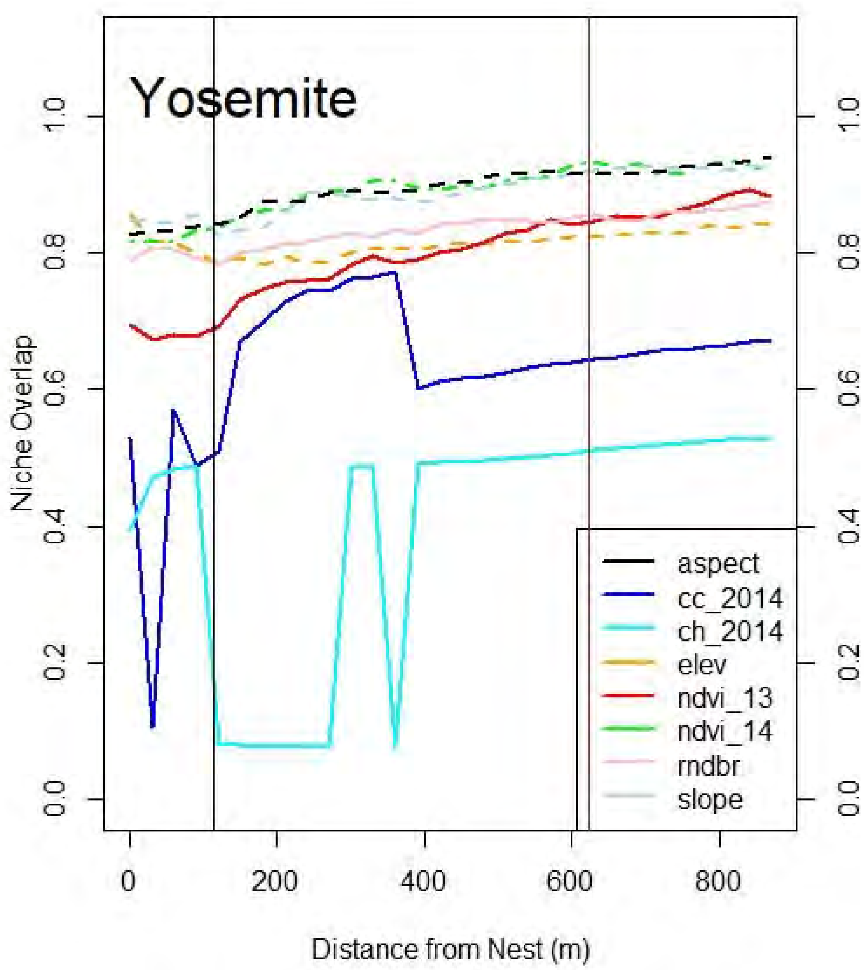

Figure 2: Niche-overlap modeling results for pre and post fire, Landsat-based metrics: *The metrics are defined as cc_2014 = Canopy cover 2014, Ch_2014 = Canopy height 2014. The patterns observed in the niche overlap modeling is likely attributed to the factored nature of the data and the coarseness/patchiness of the layers.*

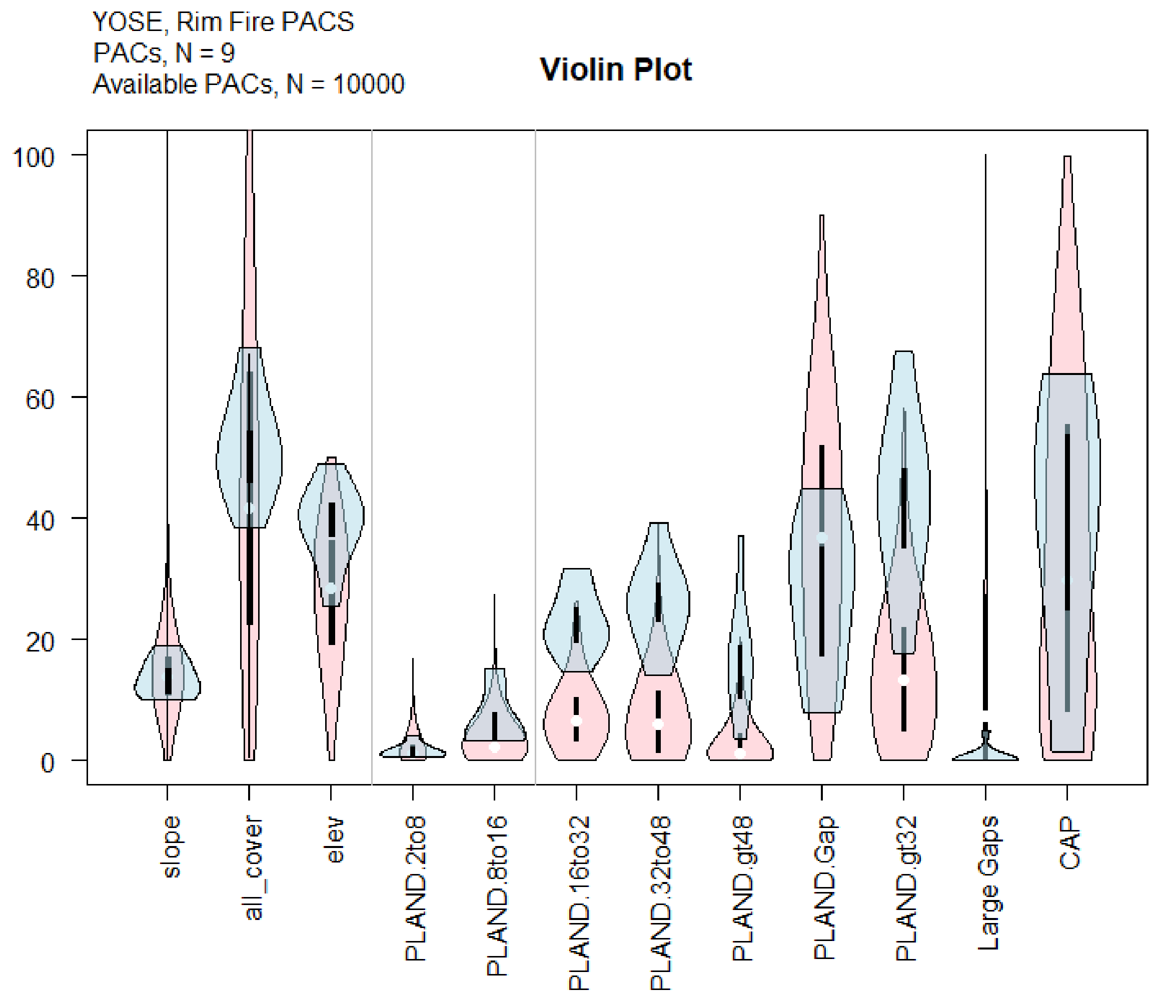

Figure 3: Violin plots of frequency of lidar and Landsat based metrics for nesting locations in the Rim fire portion of Yosemite National Park. *The pink frequencies represent the distribution of values for each metric for the 10,000 samples of the random available potential habitat, and the blue frequencies represent the distribution of values for each of the metrics of the nine nesting locations, respectively.*

Table 1: Lidar-based Canopy Structure and Topographic Metrics[4]

Selected Metrics	Landsat-based Metric	Lidar-based Metric	Niche Overlap at X Distance	Niche Overlap Rank
Selected		All canopy cover above 2m from the ground (all_cover_above2_30METERS.img)	0.471	17
Selected		95th percentile of height of all lidar returns above 2m from the ground-height of tallest portion of overstory canopy (elev_P95_2plus_30METERS.img)	0.544	50
Selected		The percent of area of canopy cover between 16 and 32m in height (PLAND.16to32_90m.img)	0.745	227
Selected		The percent of area of canopy cover between 2 and 8m in height (PLAND.2to8_90m.img)	0.622	229
Selected		The percent of area of canopy cover between 32 and 48m in height (PLAND.32to48_90m.img)	0.490	231
Selected		The percent of area of canopy cover between 8 to 16m in height (PLAND.8to16_90m.img)	0.777	233
Selected		The percent of area of canopy cover between 48 to 90m in height (PLAND.gt48_90m.img)	0.420	239
Selected		The percent of area not covered by vegetation, Gaps in total canopy area (PLAND.Gap_90m.img)	0.410	237
Selected	Relative differenced normalized burn ration (RdNBR)	Relative differenced normalized burn ration (RdNBR based on satellite, analyzed with lidar-based metrics)		
Selected	Aspect			
Selected	Canopy Cover 2014			
Selected	Canopy Height 2014			
Selected	Ground Elevation			
Selected	Normalized Difference Vegetation Index (NDVI) 2013			
Selected	NDVI 2014			
Selected	Slope			
		1000M_tpi_tpi_30METERS.img	0.518	373
		135M_topo_aspect_30METERS.img	0.832	374
		135M_topo_curvature_30METERS.img	0.663	375
		135M_topo_elevation_30METERS.img	0.737	376
		135M_topo_plancurv_30METERS.img	0.693	377
		135M_topo_profilecurv_30METERS.img	0.721	378
		135M_topo_slope_30METERS.img	0.770	379
		135M_topo_sri_30METERS.img	0.822	380
		15M_topo_aspect_30METERS.img	0.834	381
		15M_topo_curvature_30METERS.img	0.894	382
		15M_topo_elevation_30METERS.img	0.737	383
		15M_topo_plancurv_30METERS.img	0.910	384

[4] Many lidar metrics are highly correlated (for example, alternative methods for calculating canopy cover). For highly correlated metrics, the best performing metric was incorporated into the model.

		15M_topo_profilecurv_30METERS.img	0.914	385
		15M_topo_slope_30METERS.img	0.869	386
		15M_topo_sri_30METERS.img	0.894	387
		1st_cnt_above_mean_30METERS.img	0.532	1
		1st_cnt_above_mean_30METERS.img.	0.532	NA
		1st_cnt_above_mode_30METERS.img	0.609	2
		1st_cnt_above2_30METERS.img	0.507	3
		1st_cover_above_mean_30METERS.img	0.527	4
		1st_cover_above_mode_30METERS.img	0.646	5
		1st_cover_above2_30METERS.img	0.459	6
		2000M_tpi_tpi_30METERS.img	0.631	388
		200M_tpi_tpi_30METERS.img	0.714	389
		270M_topo_aspect_30METERS.img	0.779	390
		270M_topo_curvature_30METERS.img	0.522	391
		270M_topo_elevation_30METERS.img	0.737	392
		270M_topo_plancurv_30METERS.img	0.559	393
		270M_topo_profilecurv_30METERS.img	0.564	394
		270M_topo_slope_30METERS.img	0.783	395
		270M_topo_sri_30METERS.img	0.815	396
		4000M_tpi_tpi_30METERS.img	0.722	397
		45M_topo_aspect_30METERS.img	0.853	398
		45M_topo_curvature_30METERS.img	0.804	399
		45M_topo_elevation_30METERS.img	0.737	400
		45M_topo_plancurv_30METERS.img	0.837	401
		45M_topo_profilecurv_30METERS.img	0.837	402
		45M_topo_slope_30METERS.img	0.818	403
		45M_topo_sri_30METERS.img	0.877	404
		500M_tpi_tpi_30METERS.img	0.533	405
		all_1st_cover_above_mean_30METERS.img	0.527	7
		all_1st_cover_above_mode_30METERS.img	0.643	8
		all_1st_cover_above2_30METERS.img	0.479	9
		all_cnt_2plus_30METERS.img	0.499	10
		all_cnt_30METERS.img	0.728	11
		all_cnt_above_mean_30METERS.img	0.516	12
		all_cnt_above_mode_30METERS.img	0.609	13
		all_cnt_above2_30METERS.img	0.500	14
		all_cover_above_mean_30METERS.img	0.515	15
		all_cover_above_mode_30METERS.img	0.685	16
		CA.16to32_30m.img	0.776	184
		CA.16to32_90m.img	0.745	185
		CA.2to8_30m.img	0.756	186

		CA.2to8_90m.img	0.622	187
		CA.32to48_30m.img	0.589	188
		CA.32to48_90m.img	0.490	189
		CA.8to16_30m.img	0.793	190
		CA.8to16_90m.img	0.777	191
		CA.Canopy_30m.img	0.501	192
		CA.Canopy_90m.img	0.410	193
		CA.Gap_30m.img	0.501	194
		CA.Gap_90m.img	0.410	195
		CA.gt48_30m.img	0.321	196
		CA.gt48_90m.img	0.420	197
		canopy_30METERS_average_height.img	0.445	258
		canopy_30METERS_FPV.img	0.584	259
		canopy_30METERS_maximum_height.img	0.509	260
		canopy_30METERS_rumple.img	0.514	261
		canopy_30METERS_stddev_height.img	0.546	262
		elev_AAD_2plus_30METERS.img	0.567	18
		elev_ave_2plus_30METERS.img	0.592	19
		elev_canopy_relief_ratio_30METERS.img	0.819	20
		elev_cubic_mean_30METERS.img	0.571	21
		elev_CV_2plus_30METERS.img	0.859	22
		elev_IQ_2plus_30METERS.img	0.582	23
		elev_kurtosis_2plus_30METERS.img	0.855	24
		elev_L1_2plus_30METERS.img	0.609	25
		elev_L2_2plus_30METERS.img	0.547	26
		elev_L3_plus_30METERS.img	0.826	27
		elev_L4_2plus_30METERS.img	0.809	28
		elev_LCV_2plus_30METERS.img	0.872	29
		elev_Lkurtosis_2plus_30METERS.img	0.911	30
		elev_Lskewness_2plus_30METERS.img	0.883	31
		elev_MAD_median_30METERS.img	0.581	32
		elev_MAD_mode_30METERS.img	0.613	33
		elev_max_2plus_30METERS.img	0.521	34
		elev_min_2plus_30METERS.img	0.905	35
		elev_mode_2plus_30METERS.img	0.744	36
		elev_P01_2plus_30METERS.img	0.690	37
		elev_P05_2plus_30METERS.img	0.658	38
		elev_P10_2plus_30METERS.img	0.667	39
		elev_P20_2plus_30METERS.img	0.670	40
		elev_P25_2plus_30METERS.img	0.645	41
		elev_P30_2plus_30METERS.img	0.651	42

		elev_P40_2plus_30METERS.img	0.648	43
		elev_P50_2plus_30METERS.img	0.631	44
		elev_P60_2plus_30METERS.img	0.603	45
		elev_P70_2plus_30METERS.img	0.593	46
		elev_P75_2plus_30METERS.img	0.599	47
		elev_P80_2plus_30METERS.img	0.571	48
		elev_P90_2plus_30METERS.img	0.571	49
		elev_P99_2plus_30METERS.img	0.535	51
		elev_quadratic_mean_30METERS.img	0.582	52
		elev_skewness_2plus_30METERS.img	0.874	53
		elev_stddev_2plus_30METERS.img	0.550	54
		elev_variance_2plus_30METERS.img	0.549	55
		FIRST_RETURNS_1st_cnt_above_mean_30METERS.img	0.510	56
		FIRST_RETURNS_1st_cnt_above_mode_30METERS.img	0.627	57
		FIRST_RETURNS_1st_cnt_above2_30METERS.img	0.528	58
		FIRST_RETURNS_1st_cover_above_mean_30METERS.img	0.537	59
		FIRST_RETURNS_1st_cover_above_mode_30METERS.img	0.670	60
		FIRST_RETURNS_1st_cover_above2_30METERS.img	0.481	61
		FIRST_RETURNS_all_1st_cover_above_mean_30METERS.img	0.535	62
		FIRST_RETURNS_all_1st_cover_above_mode_30METERS.img	0.685	63
		FIRST_RETURNS_all_1st_cover_above2_30METERS.img	0.489	64
		FIRST_RETURNS_all_cnt_2plus_30METERS.img	0.514	65
		FIRST_RETURNS_all_cnt_30METERS.img	0.882	66
		FIRST_RETURNS_all_cnt_above_mean_30METERS.img	0.528	67
		FIRST_RETURNS_all_cnt_above_mode_30METERS.img	0.638	68
		FIRST_RETURNS_all_cnt_above2_30METERS.img	0.521	69
		FIRST_RETURNS_all_cover_above_mean_30METERS.img	0.534	70
		FIRST_RETURNS_all_cover_above_mode_30METERS.img	0.659	71
		FIRST_RETURNS_all_cover_above2_30METERS.img	0.486	72
		FIRST_RETURNS_elev_AAD_2plus_30METERS.img	0.572	73
		FIRST_RETURNS_elev_ave_2plus_30METERS.img	0.612	74
		FIRST_RETURNS_elev_canopy_relief_ratio_30METERS.img	0.837	75
		FIRST_RETURNS_elev_cubic_mean_30METERS.img	0.583	76
		FIRST_RETURNS_elev_CV_2plus_30METERS.img	0.879	77
		FIRST_RETURNS_elev_IQ_2plus_30METERS.img	0.606	78
		FIRST_RETURNS_elev_kurtosis_2plus_30METERS.img	0.875	79
		FIRST_RETURNS_elev_L1_2plus_30METERS.img	0.605	80
		FIRST_RETURNS_elev_L2_2plus_30METERS.img	0.555	81
		FIRST_RETURNS_elev_L3_plus_30METERS.img	0.832	82
		FIRST_RETURNS_elev_L4_2plus_30METERS.img	0.806	83
		FIRST_RETURNS_elev_LCV_2plus_30METERS.img	0.864	84

		FIRST_RETURNS_elev_Lkurtosis_2plus_30METERS.img	0.913	85
		FIRST_RETURNS_elev_Lskewness_2plus_30METERS.img	0.900	86
		FIRST_RETURNS_elev_MAD_median_30METERS.img	0.594	87
		FIRST_RETURNS_elev_MAD_mode_30METERS.img	0.619	88
		FIRST_RETURNS_elev_max_2plus_30METERS.img	0.531	89
		FIRST_RETURNS_elev_min_2plus_30METERS.img	0.799	90
		FIRST_RETURNS_elev_mode_2plus_30METERS.img	0.734	91
		FIRST_RETURNS_elev_P01_2plus_30METERS.img	0.699	92
		FIRST_RETURNS_elev_P05_2plus_30METERS.img	0.678	93
		FIRST_RETURNS_elev_P10_2plus_30METERS.img	0.682	94
		FIRST_RETURNS_elev_P20_2plus_30METERS.img	0.673	95
		FIRST_RETURNS_elev_P25_2plus_30METERS.img	0.680	96
		FIRST_RETURNS_elev_P30_2plus_30METERS.img	0.657	97
		FIRST_RETURNS_elev_P40_2plus_30METERS.img	0.646	98
		FIRST_RETURNS_elev_P50_2plus_30METERS.img	0.625	99
		FIRST_RETURNS_elev_P60_2plus_30METERS.img	0.624	100
		FIRST_RETURNS_elev_P70_2plus_30METERS.img	0.617	101
		FIRST_RETURNS_elev_P75_2plus_30METERS.img	0.585	102
		FIRST_RETURNS_elev_P80_2plus_30METERS.img	0.585	103
		FIRST_RETURNS_elev_P90_2plus_30METERS.img	0.558	104
		FIRST_RETURNS_elev_P95_2plus_30METERS.img	0.561	105
		FIRST_RETURNS_elev_P99_2plus_30METERS.img	0.535	106
		FIRST_RETURNS_elev_quadratic_mean_30METERS.img	0.602	107
		FIRST_RETURNS_elev_skewness_2plus_30METERS.img	0.896	108
		FIRST_RETURNS_elev_stddev_2plus_30METERS.img	0.557	109
		FIRST_RETURNS_elev_variance_2plus_30METERS.img	0.574	110
		FIRST_RETURNS_int_AAD_2plus_30METERS.img	0.583	111
		FIRST_RETURNS_int_ave_2plus_30METERS.img	0.652	112
		FIRST_RETURNS_int_CV_2plus_30METERS.img	0.745	113
		FIRST_RETURNS_int_IQ_2plus_30METERS.img	0.595	114
		FIRST_RETURNS_int_kurtosis_2plus_30METERS.img	0.617	115
		FIRST_RETURNS_int_L1_2plus_30METERS.img	0.658	116
		FIRST_RETURNS_int_L2_2plus_30METERS.img	0.587	117
		FIRST_RETURNS_int_L3_2plus_30METERS.img	0.690	118
		FIRST_RETURNS_int_L4_2plus_30METERS.img	0.722	119
		FIRST_RETURNS_int_LCV_2plus_30METERS.img	0.778	120
		FIRST_RETURNS_int_Lkurtosis_2plus_30METERS.img	0.707	121
		FIRST_RETURNS_int_Lskewness_2plus_30METERS.img	0.681	122
		FIRST_RETURNS_int_max_2plus_30METERS.img	0.619	123
		FIRST_RETURNS_int_min_2plus_30METERS.img	0.489	124
		FIRST_RETURNS_int_mode_2plus_30METERS.img	0.742	125

		FIRST_RETURNS_int_P01_2plus_30METERS.img	0.862	126
		FIRST_RETURNS_int_P05_2plus_30METERS.img	0.753	127
		FIRST_RETURNS_int_P10_2plus_30METERS.img	0.774	128
		FIRST_RETURNS_int_P20_2plus_30METERS.img	0.772	129
		FIRST_RETURNS_int_P25_2plus_30METERS.img	0.746	130
		FIRST_RETURNS_int_P30_2plus_30METERS.img	0.733	131
		FIRST_RETURNS_int_P40_2plus_30METERS.img	0.691	132
		FIRST_RETURNS_int_P50_2plus_30METERS.img	0.685	133
		FIRST_RETURNS_int_P60_2plus_30METERS.img	0.675	134
		FIRST_RETURNS_int_P70_2plus_30METERS.img	0.643	135
		FIRST_RETURNS_int_P75_2plus_30METERS.img	0.631	136
		FIRST_RETURNS_int_P80_2plus_30METERS.img	0.632	137
		FIRST_RETURNS_int_P90_2plus_30METERS.img	0.628	138
		FIRST_RETURNS_int_P95_2plus_30METERS.img	0.587	139
		FIRST_RETURNS_int_P99_2plus_30METERS.img	0.552	140
		FIRST_RETURNS_int_skewness_2plus_30METERS.img	0.661	141
		FIRST_RETURNS_int_stddev_2plus_30METERS.img	0.562	142
		FIRST_RETURNS_int_variance_2plus_30METERS.img	0.577	143
		FIRST_RETURNS_pulsecnt_30METERS.img	0.883	144
		FIRST_RETURNS_r1_cnt_2plus_30METERS.img	0.520	145
		Height.CV_30m.img	0.938	198
		Height.CV_90m.img	0.748	199
		Height.Mean_30m.img	0.583	200
		Height.Mean_90m.img	0.509	201
		Height.P25_30m.img	0.650	202
		Height.P25_90m.img	0.539	203
		Height.P50_30m.img	0.628	204
		Height.P50_90m.img	0.563	205
		Height.P75_30m.img	0.595	206
		Height.P75_90m.img	0.525	207
		Height.P95_30m.img	0.540	208
		Height.P95_90m.img	0.486	209
		Height.QuadMean_30m.img	0.575	210
		Height.QuadMean_90m.img	0.506	211
		Height.SD_30m.img	0.683	212
		Height.SD_90m.img	0.547	213
		int_AAD_2plus_30METERS.img	0.596	146
		int_ave_2plus_30METERS.img	0.659	147
		int_CV_2plus_30METERS.img	0.738	148
		int_IQ_2plus_30METERS.img	0.873	149
		int_kurtosis_2plus_30METERS.img	0.592	150

		int_L1_2plus_30METERS.img	0.670	151
		int_L2_2plus_30METERS.img	0.837	152
		int_L3_2plus_30METERS.img	0.804	153
		int_L4_2plus_30METERS.img	0.824	154
		int_LCV_2plus_30METERS.img	0.830	155
		int_Lkurtosis_2plus_30METERS.img	0.869	156
		int_Lskewness_2plus_30METERS.img	0.854	157
		int_max_2plus_30METERS.img	0.594	158
		int_min_2plus_30METERS.img	0.435	159
		int_mode_2plus_30METERS.img	0.666	160
		int_P01_2plus_30METERS.img	0.833	161
		int_P05_2plus_30METERS.img	0.867	162
		int_P10_2plus_30METERS.img	0.820	163
		int_P20_2plus_30METERS.img	0.871	164
		int_P25_2plus_30METERS.img	0.845	165
		int_P30_2plus_30METERS.img	0.835	166
		int_P40_2plus_30METERS.img	0.789	167
		int_P50_2plus_30METERS.img	0.793	168
		int_P60_2plus_30METERS.img	0.792	169
		int_P70_2plus_30METERS.img	0.780	170
		int_P75_2plus_30METERS.img	0.814	171
		int_P80_2plus_30METERS.img	0.773	172
		int_P90_2plus_30METERS.img	0.806	173
		int_P95_2plus_30METERS.img	0.809	174
		int_P99_2plus_30METERS.img	0.794	175
		int_skewness_2plus_30METERS.img	0.717	176
		int_stddev_2plus_30METERS.img	0.577	177
		int_variance_2plus_30METERS.img	0.590	178
		Ntao.16to32_30m.img	0.722	214
		Ntao.16to32_90m.img	0.706	215
		Ntao.2to8_30m.img	0.749	216
		Ntao.2to8_90m.img	0.585	217
		Ntao.32to48_30m.img	0.477	218
		Ntao.32to48_90m.img	0.491	219
		Ntao.8to16_30m.img	0.601	220
		Ntao.8to16_90m.img	0.793	221
		Ntao.Gap_30m.img	NA	222
		Ntao.Gap_90m.img	NA	223
		Ntao.gt48_30m.img	NA	224
		Ntao.gt48_90m.img	NA	225
		PLAND.16to32_30m.img	0.776	226

		PLAND.2to8_30m.img	0.756	228
		PLAND.32to48_30m.img	0.589	230
		PLAND.8to16_30m.img	0.793	232
		PLAND.Canopy_30m.img	0.501	234
		PLAND.Canopy_90m.img	0.410	235
		PLAND.Gap_30m.img	0.501	236
		PLAND.gt48_30m.img	0.321	238
		pulsecnt_30METERS.img	0.887	179
		r1_cnt_2plus_30METERS.img	0.528	180
		r2_cnt_2plus_30METERS.img	0.513	181
		r3_cnt_2plus_30METERS.img	0.513	182
		r4_cnt_2plus_30METERS.img	0.524	183
		ShannonEven.Canopyonly_30m.img	0.732	240
		ShannonEven.Canopyonly_90m.img	0.711	241
		strata_0p5to1M_CV_30METERS.img	0.880	263
		strata_0p5to1M_kurtosis_30METERS.img	0.901	264
		strata_0p5to1M_max_30METERS.img	0.769	265
		strata_0p5to1M_mean_30METERS.img	0.921	266
		strata_0p5to1M_median_30METERS.img	0.913	267
		strata_0p5to1M_min_30METERS.img	0.846	268
		strata_0p5to1M_mode_30METERS.img	0.847	269
		strata_0p5to1M_return_proportion_30METERS.img	0.773	270
		strata_0p5to1M_skewness_30METERS.img	0.917	271
		strata_0p5to1M_stddev_30METERS.img	0.916	272
		strata_0p5to1M_total_return_cnt_30METERS.img	0.833	273
		strata_0to0p5M_CV_30METERS.img	0.999	274
		strata_0to0p5M_kurtosis_30METERS.img	0.932	275
		strata_0to0p5M_max_30METERS.img	0.832	276
		strata_0to0p5M_mean_30METERS.img	0.887	277
		strata_0to0p5M_median_30METERS.img	0.854	278
		strata_0to0p5M_min_30METERS.img	0.875	279
		strata_0to0p5M_mode_30METERS.img	0.845	280
		strata_0to0p5M_return_proportion_30METERS.img	0.496	281
		strata_0to0p5M_skewness_30METERS.img	0.853	282
		strata_0to0p5M_stddev_30METERS.img	0.860	283
		strata_0to0p5M_total_return_cnt_30METERS.img	0.665	284
		strata_16to32M_CV_30METERS.img	0.761	285
		strata_16to32M_kurtosis_30METERS.img	0.809	286
		strata_16to32M_max_30METERS.img	0.433	287
		strata_16to32M_mean_30METERS.img	0.725	288
		strata_16to32M_median_30METERS.img	0.753	289

		strata_16to32M_min_30METERS.img	0.893	290
		strata_16to32M_mode_30METERS.img	0.782	291
		strata_16to32M_return_proportion_30METERS.img	0.541	292
		strata_16to32M_skewness_30METERS.img	0.809	293
		strata_16to32M_stddev_30METERS.img	0.700	294
		strata_16to32M_total_return_cnt_30METERS.img	0.530	295
		strata_1to2M_CV_30METERS.img	0.898	296
		strata_1to2M_kurtosis_30METERS.img	0.890	297
		strata_1to2M_max_30METERS.img	0.763	298
		strata_1to2M_mean_30METERS.img	0.941	299
		strata_1to2M_median_30METERS.img	0.949	300
		strata_1to2M_min_30METERS.img	0.777	301
		strata_1to2M_mode_30METERS.img	0.808	302
		strata_1to2M_return_proportion_30METERS.img	0.800	303
		strata_1to2M_skewness_30METERS.img	0.973	304
		strata_1to2M_stddev_30METERS.img	0.894	305
		strata_1to2M_total_return_cnt_30METERS.img	0.839	306
		strata_2to4M_CV_30METERS.img	0.870	307
		strata_2to4M_kurtosis_30METERS.img	0.881	308
		strata_2to4M_max_30METERS.img	0.864	309
		strata_2to4M_mean_30METERS.img	0.810	310
		strata_2to4M_median_30METERS.img	0.815	311
		strata_2to4M_min_30METERS.img	0.759	312
		strata_2to4M_mode_30METERS.img	0.829	313
		strata_2to4M_return_proportion_30METERS.img	0.811	314
		strata_2to4M_skewness_30METERS.img	0.830	315
		strata_2to4M_stddev_30METERS.img	0.907	316
		strata_2to4M_total_return_cnt_30METERS.img	0.802	317
		strata_32to48M_CV_30METERS.img	0.696	318
		strata_32to48M_kurtosis_30METERS.img	0.870	319
		strata_32to48M_max_30METERS.img	0.493	320
		strata_32to48M_mean_30METERS.img	0.714	321
		strata_32to48M_median_30METERS.img	0.729	322
		strata_32to48M_min_30METERS.img	0.900	323
		strata_32to48M_mode_30METERS.img	0.756	324
		strata_32to48M_return_proportion_30METERS.img	0.491	325
		strata_32to48M_skewness_30METERS.img	0.874	326
		strata_32to48M_stddev_30METERS.img	0.700	327
		strata_32to48M_total_return_cnt_30METERS.img	0.477	328
		strata_48to64M_CV_30METERS.img	0.827	329
		strata_48to64M_kurtosis_30METERS.img	0.933	330

		strata_48to64M_max_30METERS.img	0.797	331
		strata_48to64M_mean_30METERS.img	0.822	332
		strata_48to64M_median_30METERS.img	0.831	333
		strata_48to64M_min_30METERS.img	0.818	334
		strata_48to64M_mode_30METERS.img	0.793	335
		strata_48to64M_return_proportion_30METERS.img	0.263	336
		strata_48to64M_skewness_30METERS.img	0.939	337
		strata_48to64M_stddev_30METERS.img	0.824	338
		strata_48to64M_total_return_cnt_30METERS.img	0.323	339
		strata_4to8M_CV_30METERS.img	0.919	340
		strata_4to8M_kurtosis_30METERS.img	0.902	341
		strata_4to8M_max_30METERS.img	0.863	342
		strata_4to8M_mean_30METERS.img	0.825	343
		strata_4to8M_median_30METERS.img	0.836	344
		strata_4to8M_min_30METERS.img	0.894	345
		strata_4to8M_mode_30METERS.img	0.842	346
		strata_4to8M_return_proportion_30METERS.img	0.815	347
		strata_4to8M_skewness_30METERS.img	0.842	348
		strata_4to8M_stddev_30METERS.img	0.894	349
		strata_4to8M_total_return_cnt_30METERS.img	0.780	350
		strata_64M_plus_CV_30METERS.img	0.803	351
		strata_64M_plus_kurtosis_30METERS.img	0.866	352
		strata_64M_plus_max_30METERS.img	0.772	353
		strata_64M_plus_mean_30METERS.img	0.795	354
		strata_64M_plus_median_30METERS.img	0.832	355
		strata_64M_plus_min_30METERS.img	0.922	356
		strata_64M_plus_mode_30METERS.img	0.791	357
		strata_64M_plus_return_proportion_30METERS.img	0.328	358
		strata_64M_plus_skewness_30METERS.img	0.921	359
		strata_64M_plus_stddev_30METERS.img	0.801	360
		strata_64M_plus_total_return_cnt_30METERS.img	0.436	361
		strata_8to16M_CV_30METERS.img	0.852	362
		strata_8to16M_kurtosis_30METERS.img	0.841	363
		strata_8to16M_max_30METERS.img	0.730	364
		strata_8to16M_mean_30METERS.img	0.786	365
		strata_8to16M_median_30METERS.img	0.803	366
		strata_8to16M_min_30METERS.img	0.895	367
		strata_8to16M_mode_30METERS.img	0.830	368
		strata_8to16M_return_proportion_30METERS.img	0.740	369
		strata_8to16M_skewness_30METERS.img	0.824	370
		strata_8to16M_stddev_30METERS.img	0.801	371

		strata_8to16M_total_return_cnt_30METERS.img	0.666	372
		TotalArea_30m.img	NA	242
		TotalArea_90m.img	NA	243
		Volume.16to32_30m.img	0.776	244
		Volume.16to32_90m.img	0.734	245
		Volume.2to8_30m.img	0.765	246
		Volume.2to8_90m.img	0.633	247
		Volume.32to48_30m.img	0.587	248
		Volume.32to48_90m.img	0.488	249
		Volume.8to16_30m.img	0.796	250
		Volume.8to16_90m.img	0.783	251
		Volume.Canopy_30m.img	0.459	252
		Volume.Canopy_90m.img	0.395	253
		Volume.Gap_30m.img	NA	254
		Volume.Gap_90m.img	NA	255
		Volume.gt48_30m.img	0.320	256
		Volume.gt48_90m.img	0.415	257